AIAA JOURNAL
Vol. 33, No. 1, January 1995

Method for Determining Minimum-Order Mass and Stiffness Matrices from Modal Test Data

K. F. Alvin,* L. D. Peterson,† and K. C. Park‡
University of Colorado, Boulder, Colorado 80309

A new method for determining mass and stiffness matrices from modal test data is presented. The method builds on the identified modes and the mass-normalized mode shapes at the sensor locations and is not limited by either the number of driving points or measurement points, and so it is applicable to most general test settings. A mixed coordinate basis is defined for the mass and stiffness matrices which is analogous to the Craig-Bampton component mode synthesis method for finite element models. The resultant mass and stiffness are of minimal order necessary to span the measured modes, and the resulting generalized coordinates provide an objective basis for the test-derived matrices to be used as if they are component mode-synthesized finite element matrices. Inclusion of rigid-body modes and the relationship of the new method to traditional physical parameter computations based on mobility curves is considered. Examples of the method as applied to numerical and experimental data are provided.

I. Introduction

THE primary objective of modal testing of structures is to validate the homogeneous form of the governing linear differential equations of motion in terms of the dominant undamped modes of vibration.[1] Naturally, there is only a finite number of points on the structure for which data can be collected, and these points are generally a small subset of the total degrees of freedom (DOF) in a reasonably accurate finite element model of the structure. In fact, the number of measurement points may also be less than the total number of vibrational modes identified in the test, especially when utilizing modern instrumentation with high sampling rates and powerful, inexpensive scientific workstations for data analysis. Therefore, if l sensors are used to identify modal data for n modes, where $n > l$, there is not a unique model of the classical mass/stiffness form with physical DOF which possesses order-n dynamics given only l spatial measurement points.

Much research in recent years has focused on methods for correlation or reconciliation of finite element models which inherently possess very large-order dynamics to the limited sensor and frequency data obtained from modal testing.[2–4] The primary advantage of this approach is that the measured data can be related back to physical design parameters of the system, resulting in a model which not only possesses the observed modal characteristics but will predict internal stress levels and sensitivity to further design changes as well. The drawback, however, is that these models must retain far higher numbers of degrees of freedom than can be correlated in test, and it is exactly the high-order localized uncorrelated behavior which is influential in specific model predictions such as stress distribution. Thus, although these models may be superior in most ways to unverified finite element models, there can be a tendency to trust their behavior in all cases when only their low-frequency global characteristics have been correlated.

An alternative approach is to directly construct (i.e., calculate) mass and stiffness from the modal parameters identified by test. The resulting matrices will then express only the behavior measured and not interpolate further degrees of complexity. The primary goal of the present paper is to investigate direct solutions to the inverse vibration problem when the number of sensors l is less than the number of identified modes n. We will show that mass and stiffness matrices of dimension l, referring to the measured DOF, can be found from the n identified modes. These matrices are effectively reduced properties of the system, condensing n modal DOF into l physical DOF, and the reduced matrices are directly related to classical model reduction, namely, the so-called Guyan method. Like the Guyan reduction technique for finite element models, a characteristic of the present procedure is that the low-frequency modes are more accurately preserved by the condensation of the modal spectrum, and, in the limit as rigid-body modes are included in the coordinate reduction, they are exactly preserved. The present procedure can also handle cases where l is greater than n by user selection of master and slave degrees of freedom which are related by multipoint constraints.

One serious drawback of reduced physical matrices is that they condense the identified dynamics from a test into a smaller dimensional space. Thus, the measured eigenvalues and eigenvectors are not preserved by the resultant mass and stiffness matrices, and the model defined by the reduced matrices is not equivalent to the test in terms of the measured transfer functions. To address this issue, we endeavor to derive mass and stiffness matrices which possess both the physical nature of the previous reduced parameters and yet preserve the full eigenspectrum as measured in a test. If the mass and stiffness are determined strictly from a test, as opposed to the common problem of large-order finite element model correlation, then the resultant matrices will be of minimum order to express the identified modes. In fact, these minimum-order coefficients for the second-order structural dynamic equations will, when cast into state space form, lead to a realization of the system transfer functions fully equivalent to the system realization used to derive the modal data.

The coordinate set chosen for the derivation of minimal-order mass and stiffness consists of the measured physical DOF augmented by a set of generalized DOF which are specifically modal coordinates of the residual dynamics. The residual dynamic matrix is the difference between the measured (i.e., identified) eigenvalues of the modes and the projection of the reduced stiffness through the measured mode shapes. A singular value decomposition of the residual dynamic matrix is then used to determine the rank deficiency of the reduced stiffness, and a minimum-order augmentation of the mode shapes using the orthonormal vectors of the singular values is performed to find the new minimal-order stiffness and mass matrices. Finally, the augmented portions of the new stiffness and mass matrices are diagonalized such that the augmented DOF possess the desired modal orientation for the residual dynamics. This method of representation is similar to the Craig-Bampton component mode synthesis method for finite element models, which is popular among structural dynamicists.

Received Oct. 26, 1993; revision received Aug. 2, 1994; accepted for publication Aug. 3, 1994.

*Research Associate, Department of Aerospace Engineering Sciences and Center for Space Structures and Controls. Member AIAA.

†Assistant Professor, Department of Aerospace Engineering Sciences and Center for Space Structures and Controls. Senior Member AIAA.

‡Professor, Department of Aerospace Engineering Sciences and Center for Space Structures and Controls. Associate Fellow AIAA.

The remainder of the paper is organized as follows. Section II presents a method for determining reduced stiffness and mass matrices from test-measured modal parameters and its relationship to the Guyan reduction technique for finite element analysis. Section III extends this technique by determining minimal-order stiffness and mass matrices which fully preserve the measured eigenvalues and eigenvectors. Section IV reviews methods for determining estimates of the normal modal parameters of the structure via modern modal testing and data reduction. Finally, Sec. V presents examples of the present methods utilizing both simulated and experimental data.

II. Reduced Mass and Stiffness Matrices from Identified Modal Parameters

Recent work in the area of structural identification has included the determination of mass and stiffness matrices directly from continuous time system realizations.[5] A major drawback to this approach, however, is that it requires the dimension of the physical model to be equivalent to the number of second-order states, implying that the number of independent sensors measured are equal to the number of identified modes. A more practical approach is to enrich the computed mass and stiffness matrices with the complete set of measured modes, independent of the number of sensors. This allows the resulting mass and stiffness to express contributions of all of the modes observable from the available sensors. We begin by developing the concept of reduced mass and stiffness matrices, which are defined with respect to only the set (or subset) of sensor DOF.

A. Reduced-Order Mass and Stiffness Matrices

If we partition the DOF of a large-order structural dynamics model such as those obtained from finite element discretization into a set m which is measured, and its complement i, we have

$$\begin{bmatrix} M_{mm} & M_{mi} \\ M_{mi}^T & M_{ii} \end{bmatrix} \begin{Bmatrix} \ddot{q}_m(t) \\ \ddot{q}_i(t) \end{Bmatrix} + \begin{bmatrix} \mathcal{D}_{mm} & \mathcal{D}_{mi} \\ \mathcal{D}_{mi}^T & \mathcal{D}_{ii} \end{bmatrix} \begin{Bmatrix} \dot{q}_m(t) \\ \dot{q}_i(t) \end{Bmatrix} + \begin{bmatrix} K_{mm} & K_{mi} \\ K_{mi}^T & K_{ii} \end{bmatrix} \begin{Bmatrix} q_m(t) \\ q_i(t) \end{Bmatrix} = \begin{bmatrix} \hat{B}_m \\ \hat{B}_i \end{bmatrix} f(t) \tag{1}$$

where the submatrices M, $\mathcal{D}$, and K are the structural mass, viscous damping, and stiffness, respectively, $q(t)$ are physical (i.e., measurable) displacement DOF, $f(t)$ is a vector of applied forces, and $\hat{B}$ maps the forces to their associated DOF. The generalized undamped eigenproblem corresponding to Eq. (1) is given as

$$\begin{gathered} K\Phi_n = M\Phi_n\Omega \\ \Phi_n^T K \Phi_n = \Omega = \operatorname{diag}\{\omega_{ni}^2, i = 1, \ldots, n\} \\ \Phi_n^T M \Phi_n = I_{n\times n} \qquad \Phi_n^T \mathcal{D} \Phi_n = \Xi \end{gathered} \tag{2}$$

where Φ_n, Ω, and Ξ are the normal mode shape, eigenvalue, and modal damping matrices, respectively.

If we solve the static equations of Eq. (1) where no forces are applied to the q_i equations ($\hat{B}_i f(t) = 0$), we have

$$q_i = -K_{ii}^{-1} K_{mi}^T q_m \tag{3}$$

and a variable reduction operator is given as

$$q = \begin{bmatrix} I \\ -K_{ii}^{-1} K_{mi}^T \end{bmatrix} q_m = \Phi_c q_m \tag{4}$$

In component mode synthesis (CMS) theory,[6] Φ_c are often termed the constraint modes, as they represent the displacement vectors of the internal degrees of freedom q_i with respect to the constraint modes, defined as the set of orthogonal unit displacements of the retained degrees of freedom q_m. Applying the transformation Eq. (4) to K, $\mathcal{D}$, and M in Eq. (1), the so-called Guyan reduced stiffness, damping, and mass[7] are

$$\begin{gathered} \bar{K} = \Phi_c^T K \Phi_c = K_{mm} - K_{mi} K_{ii}^{-1} K_{mi}^T \\ \bar{\mathcal{D}} = \Phi_c^T \mathcal{D} \Phi_c \qquad \bar{M} = \Phi_c^T M \Phi_c \end{gathered} \tag{5}$$

The resultant model clearly no longer possesses the large-order dynamics of K and M, but preserves the general behavior of the larger eigenproblem for the lowest modes and modes which are strongly influenced by the retained degrees of freedom. In fact, this procedure is exactly correct for static analysis under the aforementioned assumptions and for dynamic analysis in which the mass associated with the internal degrees of freedom is negligible. We further note that the Guyan reduction concept is really the idea of applying the static constraint modes transformation Φ_c to reduce the mass and damping matrices, as the concept of static condensation of the stiffness was employed previously in static matrix structural analysis.

We now wish to show an alternative representation of the Guyan reduction in terms of the normal modes Eq. (2) of the full-order system. We begin by assuming that the measured modes from test completely span the dynamics of Eq. (1), such that the model representation in modal coordinates is a completely equivalent realization. If we express the physical degrees of freedom $q(t)$ in terms of the normal modal variables $\eta(t)$, we have the transformation

$$q(t) = \Phi_n \eta(t) = \begin{bmatrix} \Phi_m \\ \Phi_i \end{bmatrix} \eta(t) \tag{6}$$

where Φ_m, Φ_i are partitions of the eigenvectors at the measured and unmeasured (i.e. internal) degrees of freedom, respectively. Using Eq. (2) and assuming no rigid-body modes such that Ω is nonsingular, the inverse vibration problem can be solved as

$$\begin{aligned} K^{-1} &= \Phi_n \Omega^{-1} \Phi_n^T \\ M^{-1} &= \Phi_n \Phi_n^T \end{aligned} \tag{7}$$

Using the partitions of K as in Eq. (1), the inverse of K can also be written symbolically as

$$K^{-1} = \begin{bmatrix} \bar{K}^{-1} & -\bar{K}^{-1} K_{mi} K_{ii}^{-1} \\ -K_{ii}^{-1} K_{mi}^T \bar{K}^{-1} & K_{ii}^{-1}\left(I + K_{mi}^T \bar{K}^{-1} K_{mi} K_{ii}^{-1}\right) \end{bmatrix} \tag{8}$$

where $\bar{K}$ is the Schur complement of K_{ii} in K and is equivalent to the statically condensed stiffness as given in Eq. (5). Furthermore, using the partitions of Φ_n in Eq. (6) together with Eq. (7), we have

$$K^{-1} = \begin{bmatrix} \Phi_m \Omega^{-1} \Phi_m^T & \Phi_m \Omega^{-1} \Phi_i^T \\ \Phi_i \Omega^{-1} \Phi_m^T & \Phi_i \Omega^{-1} \Phi_i^T \end{bmatrix} \tag{9}$$

Thus, comparing Eqs. (8) and (9), the Guyan-reduced stiffness matrix with respect to the measured test degrees of freedom is found as

$$\bar{K} = \left[\Phi_m \Omega^{-1} \Phi_m^T\right]^{-1} \tag{10}$$

To determine the reduced mass, a slightly different calculation is required, as from Eq. (5) $\bar{M}$ has combinations of mass and stiffness. We write the full-order mass M as

$$M = KK^{-1}MK^{-1}K$$

Expressing K^{-1} in modal terms from Eq. (7)

$$\begin{aligned} M &= K\Phi_n\Omega^{-1}\left(\Phi_n^T M \Phi_n\right)\Omega^{-1}\Phi_n^T K \\ &= K\Phi_n\Omega^{-2}\Phi_n^T K \end{aligned} \tag{11}$$

Then, applying the Guyan transformation to both sides, we have

$$\begin{gathered} \bar{M} = \Phi_c^T M \Phi_c = \Phi_c^T K \Phi_n \Omega^{-2} \Phi_n^T K \Phi_c \\ \bar{M} = [\bar{K} \quad 0] \begin{bmatrix} \Phi_m \\ \Phi_i \end{bmatrix} \Omega^{-2} \begin{bmatrix} \Phi_m^T & \Phi_i^T \end{bmatrix} \begin{bmatrix} \bar{K} \\ 0 \end{bmatrix} \\ \bar{M} = \bar{K} \Phi_m \Omega^{-2} \Phi_m^T \bar{K} \end{gathered} \tag{12}$$

Therefore, $\bar{M}$ as calculated in Eq. (12) possesses the qualities of the statically condensed mass as opposed to $(\Phi_m \Phi_m^T)^{-1}$, which gives just the Schur complement of M_{ii} in M. Note that when Φ_m spans

the modes completely (Φ_m nonsingular, number of sensors equal to number of modes), Eq. (12) simplifies to

$$\begin{aligned}\bar{M} &= \Phi_m^{-T}\Omega\Phi_m^{-1}\Phi_m\Omega^{-2}\Phi_m^T\Phi_m^{-T}\Omega\Phi_m^{-1} \\ &= \Phi_m^{-T}\Phi_m^{-1} = \left(\Phi_m\Phi_m^T\right)^{-1}\end{aligned} \tag{13}$$

which is consistent with Eq. (7), since having a full space of sensors implies that $\Phi_m = \Phi_n$. Similarly, we can find the Guyan-reduced damping matrix $\bar{\mathcal{D}}$ as

$$\bar{\mathcal{D}} = \bar{K}\Phi_m\Omega^{-1}\Xi\Omega^{-1}\Phi_m^T\bar{K} \tag{14}$$

Thus, the reduced system matrices given by Eqs. (10), (12) and (14) are theoretically consistent with the Guyan reduction in the limit as the full eigenspectrum of Eq. (1) is measured. Note, however, that although the finite element-based condensation requires knowledge of the physical properties of the eliminated DOF, the modal parameter-based condensation is a function only of the partition of the mode shapes at the measured locations and, thus, can be directly identified from the measured test data.

B. Incorporation of Rigid-Body Modes

Because the computation of the reduced stiffness Eq. (10) requires Ω^{-1}, incorporation of purely rigid-body modes, for which $\omega_{ni} = 0$, into the reduced stiffness requires a modification to the present procedure. Let Φ_m and Ω be partitioned into rigid-body and flexible modes, viz.,

$$\begin{aligned}\Phi_m &= [\Phi_{mr} \quad \Phi_{mf}] \\ \Omega &= \begin{bmatrix} 0 & 0 \\ 0 & \Omega_f \end{bmatrix}\end{aligned} \tag{15}$$

where Ω_f is nonsingular and Φ_m is mass normalized. Then, let us define a new stiffness matrix $\bar{K}_f$ as the inverse of the structural flexibility using only the contribution of the flexible modes, that is,

$$\bar{K}_f^{-1} = \Phi_{mf}\Omega_f^{-1}\Phi_{mf}^T \tag{16}$$

Then the correct reduced stiffness can be expressed symbolically as

$$\bar{K} = \lim_{\epsilon\to 0}\left(\bar{K}_f^{-1} + \frac{1}{\epsilon}\Phi_{mr}\Phi_{mr}^T\right)^{-1} \tag{17}$$

Expanding the right-hand side and simplifying, we have

$$\begin{aligned}\bar{K} = \bar{K}_f - \lim_{\epsilon\to 0}\bar{K}_f\Phi_{mr}\Bigg(&\frac{1}{\epsilon}I - \frac{1}{\epsilon^2}\Phi_{mr}^T\bar{K}_f\Phi_{mr} \\ &+ \frac{1}{\epsilon^3}\left(\Phi_{mr}^T\bar{K}_f\Phi_{mr}\right)^2 - \cdots\Bigg)\Phi_{mr}^T\bar{K}_f\end{aligned} \tag{18}$$

However, the right-hand side simplifies further by noting that

$$\begin{aligned}\left(\epsilon I + \Phi_{mr}^T\bar{K}_f\Phi_{mr}\right)^{-1} = &\frac{1}{\epsilon}I - \frac{1}{\epsilon^2}\Phi_{mr}^T\bar{K}_f\Phi_{mr} \\ &+ \frac{1}{\epsilon^3}\left(\Phi_{mr}^T\bar{K}_f\Phi_{mr}\right)^2 - \cdots\end{aligned} \tag{19}$$

Therefore, substituting Eq. (19) in Eq. (18) and letting $\epsilon \to 0$, we have

$$\bar{K} = \bar{K}_f - \bar{K}_f\Phi_{mr}\left(\Phi_{mr}^T\bar{K}_f\Phi_{mr}\right)^{-1}\Phi_{mr}^T\bar{K}_f \tag{20}$$

This result [Eq. (20)] provides an expression for incorporation of rigid-body modes which avoids the inversion of a singular eigenvalue matrix. By inspection, Eq. (20) is equivalent to a rank reduction of $\bar{K}_f$ in the given rigid-body directions Φ_{mr}. Evaluating the rigid-body behavior, we have

$$\begin{aligned}\Phi_{mr}^T\bar{K}\Phi_{mr} = &\Phi_{mr}^T\bar{K}_f\Phi_{mr} \\ &- \Phi_{mr}^T\bar{K}_f\Phi_{mr}\left(\Phi_{mr}^T\bar{K}_f\Phi_{mr}\right)^{-1}\Phi_{mr}^T\bar{K}_f\Phi_{mr} \\ &= 0\end{aligned} \tag{21}$$

Thus, the rigid-body modes are exactly preserved by the reduced stiffness $\bar{K}$. Note that the present procedure for the inclusion of rigid-body modes was developed directly from Eq. (10). Therefore, like the Guyan reduction technique, the present procedure generally preserves the lowest frequency modes and exactly preserves the rigid-body modes. Furthermore, from Eq. (20) and the fact that $\bar{K}_f$ is positive definite, $\bar{K}$ is positive definite in directions orthogonal to Φ_{mr} through $\bar{K}_f$, thus ensuring that it is positive semidefinite. Finally, following an similar approach, the reduced mass $\bar{M}$ with rigid-body modes is given as

$$\bar{M} = \bar{K}\Phi_{mf}\Omega_f^{-2}\Phi_{mf}^T\bar{K} + \bar{K}_f\Phi_{mr}\left(\Phi_{mr}^T\bar{K}_f\Phi_{mr}\right)^{-2}\Phi_{mr}^T\bar{K}_f \tag{22}$$

where $\bar{K}_f$ is given by Eq. (16), and $\bar{K}$ is the correct reduced stiffness including rigid-body modes given by Eq. (20). Evaluating the rigid-body behavior of $\bar{M}$ and noting the $\bar{K}\Phi_{mr} = 0$ from Eq. (21), we have

$$\begin{aligned}\Phi_{mr}^T\bar{M}\Phi_{mr} &= 0 + \Phi_{mr}^T\bar{K}_f\Phi_{mr}\left(\Phi_{mr}^T\bar{K}_f\Phi_{mr}\right)^{-2}\Phi_{mr}^T\bar{K}_f\Phi_{mr} \\ &= I_{r\times r}\end{aligned} \tag{23}$$

Thus, $\bar{M}$ as calculated from Eq. (22) is not only positive-definite whereas $\bar{K}$ is positive semidefinite, but, in fact, correctly preserves the mass orthonormalization of the mode shapes Φ_{mr}. Hence, from Eqs. (20) and (22) $\bar{K}$ and $\bar{M}$ together preserve the rigid-body modes defined by Φ_{mr}.

It should be noted that, whereas the flexible modal properties can be determined via modal testing, as will be reviewed in Sec. IV, the rigid-body modes are more likely obtained via analytical synthesis. Determination of the rigid-body mode shapes, however, require only knowledge of the spatial locations of the modal sensors and the overall rigid-body mass properties of the system (for the required mass normalization of the mode shapes).

C. Relationship of Reduced Measured Stiffness to Mobility Parameters

Finally, the reduced stiffness $\bar{K}$ is also an expression of the mobility curve-based stiffness parameters, the so-called system receptance.[1] From Eq. (1), the frequency domain transfer function matrix $\mathcal{H}_d(\omega)$, where $y(\omega) = \mathcal{H}(\omega)u(\omega)$, is given for displacement sensing by

$$\mathcal{H}_d(\omega) = H_d\left(K + i\omega\mathcal{D} - \omega^2 M\right)^{-1}\hat{B} \tag{24}$$

Then, assuming actuators and sensors at physical DOF q_m, the receptance is found by the asymptotic limit of $\mathcal{H}(\omega)$ as $\omega \to 0$, viz.,

$$\lim_{\omega\to 0}\mathcal{H}_d(\omega) = H_d K^{-1} H_d^T = \bar{K}^{-1} \tag{25}$$

We note here that $\bar{K}$ is determined from the modes of the identified model, which is generally a curve fit of much smaller dimension than is required to match the transfer function exactly. Thus, $\bar{K}$ expresses the receptance of the approximate model, rather than the test-measured transfer function matrix. That is, $\bar{K}$ is the curve-fit static asymptote, rather than the test-measured zero frequency value. This is important because generally modal test sensors have poor accuracy as $\omega \to 0$, so the reconstruction through $\bar{K}$ can be more reliable.

III. Minimum-Order Mass and Stiffness Matrices from Identified Modal Parameters

As noted in the Introduction, we base our method for a minimum-order equivalent mass and stiffness from test on the Craig-Bampton component mode synthesis method,[8] which itself is related to the statically condensed mass and stiffness of the Guyan reduction. Thus, we will use the method of determining the Guyan reduction from measured modes as reviewed in the preceding section to develop the equivalent minimum-order method. To begin, however, let us review the Craig-Bampton CMS method as applied to the finite element method. Recalling Eq. (3), in the Craig-Bampton method we represent q_i as

$$q_i = -K_{ii}^{-1}K_{mi}^T q_m + T_\xi\xi \tag{26}$$

where ξ are the augmented generalized degrees of freedom and T_ξ are the displacements of q_i with respect to unit displacements of ξ. Thus, the variable transformation is given as

$$q = \begin{bmatrix} I & 0 \\ -K_{ii}^{-1}K_{mi}^T & T_\xi \end{bmatrix} \begin{Bmatrix} q_m \\ \xi \end{Bmatrix} = T \begin{Bmatrix} q_m \\ \xi \end{Bmatrix} \tag{27}$$

and applying this to K gives

$$\hat{K} = T^T K T = \begin{bmatrix} \bar{K} & 0 \\ 0 & T_\xi^T K_{ii} T_\xi \end{bmatrix} \tag{28}$$

Thus, $\hat{K}$ is block diagonal, composed of the Guyan reduced stiffness and a residual symmetrical stiffness matrix. Note that we have not yet defined ξ as fixed interface modal coordinates of the residual structure; the form of $\hat{K}$ is a consequence of Eq. (27), which defines ξ as a subspace orthogonal to q_m through K. To uniquely define the direction of ξ, it is specified that T_ξ are the orthonormal eigenvectors of the generalized eigenproblem.

$$\begin{aligned} K_{ii} T_\xi &= M_{ii} T_\xi \Omega_\xi \\ T_\xi^T K_{ii} T_\xi &= \Omega_\xi \qquad T_\xi^T M_{ii} T_\xi = I \end{aligned} \tag{29}$$

Using Eq. (29) to fully define T_ξ, the Craig-Bampton stiffness and mass matrix is given by

$$\begin{aligned} \hat{K} &= T^T K T = \begin{bmatrix} \bar{K} & 0 \\ 0 & \Omega_\xi \end{bmatrix} \\ \hat{M} &= T^T M T = \begin{bmatrix} \bar{M} & M_c \\ M_c^T & I \end{bmatrix} \end{aligned} \tag{30}$$

where

$$M_c = M_{mi} T_\xi - K_{mi} K_{ii}^{-1} M_{ii} T_\xi \tag{31}$$

is a mass coupling between q_m and ξ, and $\bar{M}$ is the Guyan-reduced mass given by Eq. (5).

Using the results from Sec. 2, we can construct $\hat{K}$ and $\hat{M}$ from the measured modal test parameters Φ_m and Ω as follows. Partition the eigenvectors of to-be-determined matrices $\hat{K}$ and $\hat{M}$ as

$$\begin{bmatrix} \bar{K} & 0 \\ 0 & \Omega_{\text{res}} \end{bmatrix} \begin{bmatrix} \Phi_m \\ \Phi_{\text{res}} \end{bmatrix} = \hat{M} \begin{bmatrix} \Phi_m \\ \Phi_{\text{res}} \end{bmatrix} \Omega \tag{32}$$

normalized such that

$$\begin{bmatrix} \Phi_m^T & \Phi_{\text{res}}^T \end{bmatrix} \begin{bmatrix} \bar{K} & 0 \\ 0 & \Omega_{\text{res}} \end{bmatrix} \begin{bmatrix} \Phi_m \\ \Phi_{\text{res}} \end{bmatrix} = \Omega \tag{33}$$

Here, Φ_{res} are the partition of the eigenvectors of $\hat{K}$ and $\hat{M}$ relating the augmented variables ξ in Eq. (26) to the normal modal variables of the global system η. Although Φ_{res} and Ω_{res} are unknowns, together they form a dynamic residual matrix $\Delta\Omega$, which can be computed by the test-measured quantities Φ_m, Ω, viz.,

$$\Phi_{\text{res}}^T \Omega_{\text{res}} \Phi_{\text{res}} = \Omega - \Phi_m^T \left(\Phi_m \Omega^{-1} \Phi_m^T \right) \Phi_m = \Delta\Omega \tag{34}$$

where $\bar{K}$ in Eq. (33) is expressed in terms of the modal parameters using Eq. (10) or Eq. (20), the reduced order stiffness derived in Sec. II. Note now that $\Delta\Omega$ is a function solely of Φ_m and Ω, the identified mode shapes and frequencies.

The required minimal rank augmentation of q_m is determined through the dynamic residual matrix $\Delta\Omega$. To find the rank of Ω_{res} and a vector basis for Φ_{res}, we utilize a singular value decomposition (SVD) of $\Delta\Omega$, viz.,

$$PSP^T = \text{SVD}(\Delta\Omega)$$

Examination of the singular values clearly indicates the required dimension of the augmented coordinates ξ. For example, with l independent spatial measurements, $\Phi_m^T \bar{K} \Phi_m$ will be typically be of rank l, whereas Ω is rank n, and $\Phi_{\text{res}}^T \Omega_{\text{res}} \Phi_{\text{res}}$ is rank $(n - l)$. Therefore, the SVD should determine $(n-l)$ nonzero singular values for $\Delta\Omega$. It is possible, however, for the reduced matrix to exhibit some rank deficiency (for example, if flexibility mode contributions to $\bar{K}$ are rank updated to account for rigid-body modes), and so a rigorous approach should involve fully examining the singular values of $\Delta\Omega$ to determine the correct rank p,

$$\Delta\Omega = PSP^T = P_p S_p P_p^T \tag{35}$$

Having determined a basis P_p for the p augmented coordinates, we now augment Φ_m by the rows of P_p^T which span the singular values, and solve the general inverse vibration problem:

$$\begin{aligned} \begin{bmatrix} \bar{K} & 0 \\ 0 & K_{\text{res}} \end{bmatrix} &= \begin{bmatrix} \Phi_m \\ P_p^T \end{bmatrix}^{-T} \Omega \begin{bmatrix} \Phi_m \\ P_p^T \end{bmatrix}^{-1} \\ \begin{bmatrix} \tilde{M} & \tilde{M}_c \\ \tilde{M}_c^T & M_{\text{res}} \end{bmatrix} &= \left[\begin{bmatrix} \Phi_m \\ P_p^T \end{bmatrix} \begin{bmatrix} \Phi_m^T & P_p \end{bmatrix} \right]^{-1} \end{aligned} \tag{36}$$

Finally, the augmented DOF are orthonormalized for consistency with the definition of ξ by solving the generalized eigenproblem

$$\begin{aligned} K_{\text{res}} U &= M_{\text{res}} U \Omega_\xi \\ U^T K_{\text{res}} U &= \Omega_\xi \\ U^T M_{\text{res}} U &= I \end{aligned} \tag{37}$$

and performing a final transformation on the mass and stiffness matrices

$$\begin{aligned} \hat{K} &= \begin{bmatrix} I & 0 \\ 0 & U^T \end{bmatrix} \begin{bmatrix} \bar{K} & 0 \\ 0 & K_{\text{res}} \end{bmatrix} \begin{bmatrix} I & 0 \\ 0 & U \end{bmatrix} = \begin{bmatrix} \bar{K} & 0 \\ 0 & \Omega_\xi \end{bmatrix} \\ \hat{M} &= \begin{bmatrix} I & 0 \\ 0 & U^T \end{bmatrix} \begin{bmatrix} \tilde{M} & \tilde{M}_c \\ \tilde{M}_c^T & M_{\text{res}} \end{bmatrix} \begin{bmatrix} I & 0 \\ 0 & U \end{bmatrix} = \begin{bmatrix} \bar{M} & M_c \\ M_c^T & I \end{bmatrix} \end{aligned} \tag{38}$$

Thus, in a mathematical sense, $\hat{K}$ and $\hat{M}$ are an equivalent measure of the normal mode parameters as observed from the physical DOF q_m. Furthermore, this realization is unique from its definition in terms of the modal parameters of the system. This implies that both the Guyan-reduced properties and the Craig-Bampton representation are intrinsic parameters of the physical system independent of the particular finite element representation. Note also that the definition of $\hat{K}$ and $\hat{M}$ include as special cases both the modal model $[\Omega, I]$ and the physical model $[K, M]$ in the limits as the number of measured DOF varies from 0 to n.

IV. Extracting Modal Parameters from Test

In this section, we briefly review how the required modal parameters Ω and Φ_m (and Ξ for damping synthesis) can be obtained from identification of the modal test data. Generally, in modern modal testing, frequency response functions (FRF) over the bandwidth of interest for each input-output pairing are obtained through fast Fourier transform methods. Modal parameters are then obtain either by curve fitting techniques or from an equivalent system realization[9] of the data in the time or frequency domain. The eigensystem realization algorithm[10] (ERA) and polyreference[11] are two such system realization methods in the time domain which are widely used, particularly with respect to identification of structural dynamic systems. ERA will identify a minimum-order multiple-input discrete-time model to minimize the error in the reconstructed impulse time response. ERA uses numerical methods which are robust in the presence of measurement noise and can identify repeated roots using multiple-input reference FRFs. This model is then converted to a corresponding set of continuous time equations, viz.,

$$\begin{aligned} \dot{x}(t) &= Ax(t) + Bu(t) \\ y(t) &= Cx(t) + Du(t) \end{aligned} \tag{39}$$

Converting Eq. (39) into sets of decoupled first-order equations (using the eigendecomposition of A) yields the complex damped modes

and mode shapes which characterize the identified damped structural dynamics.

Determination of the normal (i.e., undamped) modal parameters Ω and Φ_m from Eq. (39) usually involves some ad-hoc approximation using the complex modal parameters. For example, in the case of proportional damping, the undamped frequency ω_{ni} and modal damping ratio ζ_i corresponding to the damped mode i are given as

$$\omega_{ni}^2 = \sigma_i^2 + \omega_i^2 \qquad \zeta_i = -(\sigma_i/\omega_{ni}) \tag{40}$$

where σ_i and ω_i are the real and imaginary parts of the complex eigenvalues of Eq. (39). For determining the normal mode shape for mode i at sensor DOF j, we can take the magnitude of the associated complex mode shape X_i, viz.,

$$\phi_{ij} = |X_{ij}|(\text{sgn}_{ij}) \tag{41}$$

where (sgn) $= \pm 1$ is determined by examining the phase angles of X_{ij}. The resulting mode shapes then must be mass-normalized using the modal participation factors of the applied forces from driving point measurements or by using an assumed mass matrix.

Recently, a general transformation-based algorithm has been developed which consistently extracts the modal parameters of second-order dynamics from the general state space Eqs. (39). The common basis-normalized structural identification (CBSI) procedure[12] obtains the correct normal (i.e., undamped) modal properties when the system damping is exactly proportional and a particular approximation in the more general damping case by a similarity transformation of the state space model to the normal modes form of the associated second-order equations of motion. CBSI also allows the identified mode shapes to objectively normalized in relation to the applied dynamic forces. For example, to determine an objective, experimental mass normalization of the eigenvectors, one or more driving point measurements (i.e., colocated actuator and sensor) are used. Details can be found in Ref. 12.

V. Numerical and Experimental Test Results

A. Three-DOF Undamped Spring-Mass System

To clearly and explicitly illustrate the steps of the mass and stiffness derivation methods presented in the preceding sections, the first example involves a simple undamped 3-DOF spring-mass system as shown in Fig. 1. This system is identified using one sensor at DOF q_2 from which all three modes are observable. The collocated input u serves as the modal applied force which enables the identified mode shapes to be experimentally mass normalized. The undamped equations of motion are given as

$$\begin{Bmatrix} \ddot{q}_1 \\ \ddot{q}_2 \\ \ddot{q}_3 \end{Bmatrix} + \begin{bmatrix} 4 & -2 & 0 \\ -2 & 4 & -2 \\ 0 & -2 & 22 \end{bmatrix} \begin{Bmatrix} q_1 \\ q_2 \\ q_3 \end{Bmatrix} = \begin{Bmatrix} 0 \\ u \\ 0 \end{Bmatrix} \tag{42}$$
$$y = q_2$$

The identified normal mode parameters of Eq. (42) are then given as

$$\Phi_m = [0.7226 \quad 0.6824 \quad -0.1104]$$
$$\Omega = \begin{bmatrix} 1.8980 & 0 & 0 \\ 0 & 5.8798 & 0 \\ 0 & 0 & 22.222 \end{bmatrix} \tag{43}$$

Thus, the reduced properties $\bar{K}$ and $\bar{M}$ from Eqs. (10) and (12) are found to be

$$\bar{K} = 2.8182 \qquad \bar{M} = 1.2583 \tag{44}$$

which are the correct Guyan-reduced stiffness and mass as given by Eq. (5). Note also that the Schur complement of M given by

$$\left(\Phi_m \Phi_m^T\right)^{-1} = 1.0000$$

is an incorrect expression for the Guyan-reduced mass as was shown analytically in Sec. II.

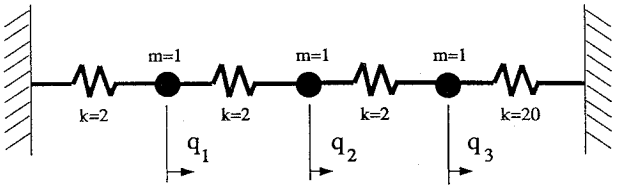

Fig. 1 Spring-mass example model.

To determine the 3-DOF minimum-order stiffness and mass, $\hat{K}$ and $\hat{M}$, respectively, we use the reduced stiffness $\bar{K}$. Applying Eq. (34), we have

$$\Delta\Omega = \begin{bmatrix} 0.4266 & -1.3896 & 0.2248 \\ -1.3896 & 4.5674 & 0.2123 \\ 0.2248 & 0.2123 & 22.188 \end{bmatrix} \tag{45}$$

Then the SVD of $\Delta\Omega$ is found to be

$$P = \begin{bmatrix} 0.0096 & -0.2917 & -0.9565 \\ 0.0113 & 0.9565 & -0.2916 \\ 0.9999 & -0.0080 & 0.0125 \end{bmatrix}$$
$$S = \begin{bmatrix} 22.192 & 0 & 0 \\ 0 & 4.989 & 0 \\ 0 & 0 & 0.0000 \end{bmatrix} \tag{46}$$

which possesses the correct rank requirement for the minimal-order augmentation. Finally, applying Eqs. (36–38), the minimum-order properties are determined, viz.,

$$\hat{K} = \begin{bmatrix} 2.8182 & 0 & 0 \\ 0 & 4.0000 & 0 \\ 0 & 0 & 22.0000 \end{bmatrix}$$
$$\hat{M} = \begin{bmatrix} 1.2583 & -0.5000 & 0.0909 \\ -0.5000 & 1.0000 & 0 \\ 0.0909 & 0 & 1.0000 \end{bmatrix} \tag{47}$$

which can be verified through Eqs. (27–30) to be consistent with the finite element-based Craig-Bampton CMS method when the boundary DOF is defined as q_2 and all fixed-interface modes are retained. This example was designed strictly to illustrate the present procedure and thus did not consider the effects of noise or modal truncation in the system identification. In the following example, these effects are considered for a more generalized structure.

B. 36-DOF Planar Truss Example

A second numerical example, shown in Fig. 2, is of a 36-DOF planar truss. Using 18 accelerometers, denoted $y1$ through $y18$ in the figure, together with three force inputs, the minimal-order mass and stiffness can be determined. To realistically simulate the corrupting effects of noise, filtering, digital sampling, and truncation of the modal spectrum, a virtual test simulator was utilized. The simulator estimates the impulse response for each input-output pairing by estimating the frequency response functions in the frequency domain through ensemble averaging. Using a uniform random force input signal for 25% of the ensemble window 10 ensembles are computed. The digital input signal is prefiltered before the analog conversion. Then the ensembles in series are applied to the continuous equations of motion and the outputs computed. Finally, both inputs and outputs are filtered at 80% of the Nyquist frequency and 1% noise added before digital sampling and storage. The sampling frequency for this example is 1000 Hz and the number of samples per ensemble is 8192. The detailed virtual simulation introduces important realism to the structural identification problem; the associated coherence functions of the estimated transfer functions are remarkably similar to those obtained in modal testing.

The system identification utilizes an efficient form of ERA[13] to determine pole information, followed by a mode discrimination process, and finally a frequency domain curve fit[14] to determine the

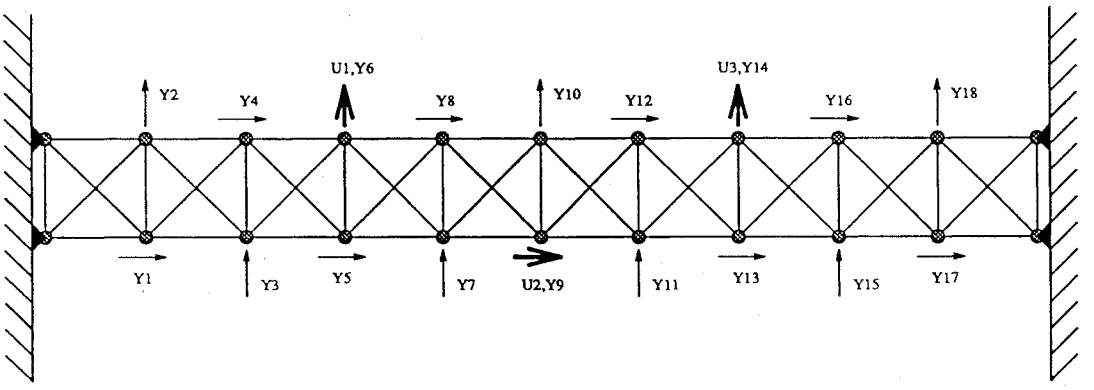

Fig. 2 Planar truss example, 36 DOF.

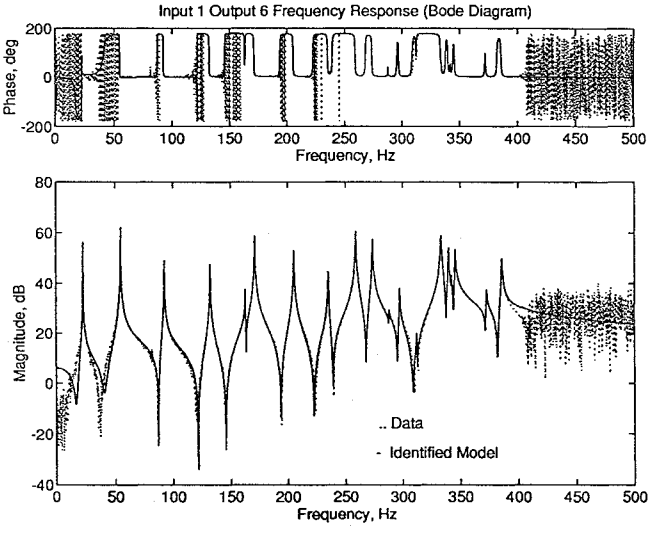

Fig. 3 Simulated data and identified model for planar truss.

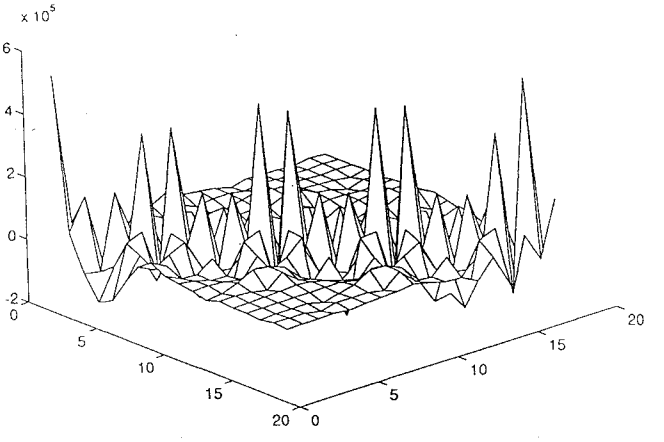

Fig. 4 Measured reduced stiffness of planar truss.

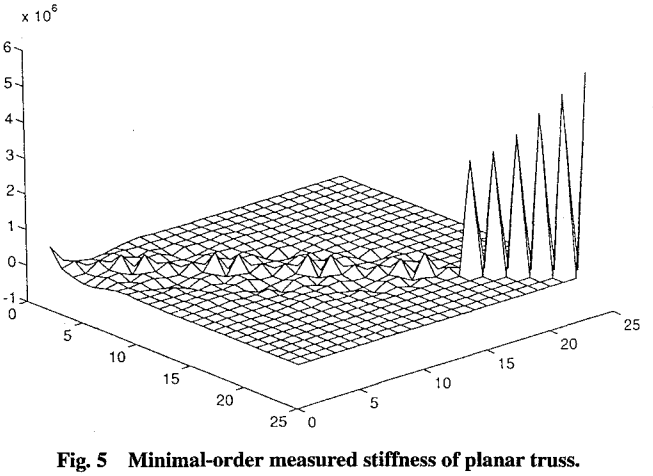

Fig. 5 Minimal-order measured stiffness of planar truss.

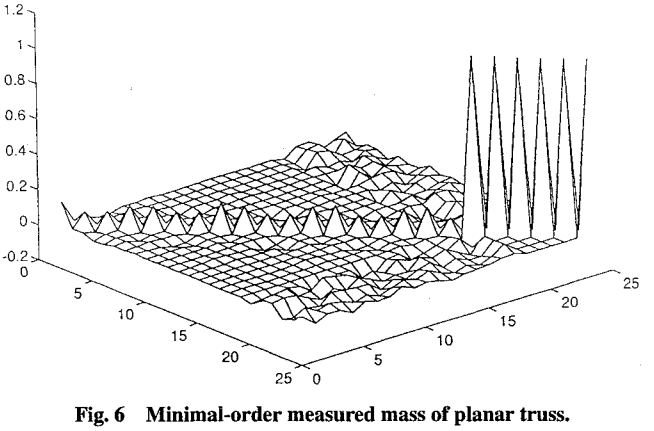

Fig. 6 Minimal-order measured mass of planar truss.

mode shapes and estimate of the residual flexibility for the measured FRFs. An example of the simulated data and the resultant system identification is shown in Fig. 3. Then, using normal modal properties as determined using the CBSI algorithm, together with the available residual flexibility terms, the reduced-order stiffness was found and is illustrated in Fig. 4. The minimal-order mass and stiffness matrices are then shown in Figs. 5 and 6. The convergence of the lowest eigenvalues of the measured stiffness as a function of the number of identified modes is illustrated in Fig. 7. The stiffness converges from a high value because it is defined as the inverse of the system flexibility at the measured degrees of freedom. Thus, when no modes are measured, the flexibility is zero, and the stiffness approaches infinity. Then, as each mode contributes flexibility to the structure, the system stiffness converges to its asymptotic form, the statically-condensed stiffness.

In Fig. 8, effective element stiffnesses in line between longitudinal sensors are contrasted using three sensor pairs. Each stiffness is effectively that of two longerons in series, plus some influence of the surrounding structure. The legend lists the sensor identification numbers from Fig. 2 which are used as the degrees of freedom of the longeron superelements. The stiffnesses are found by using only the two sensor degrees of freedom in the reduced stiffness computation, then taking the negative off-diagonal term of the 2×2 reduced element stiffness matrix as the value of the stiffness coupling between the two degrees of freedom. Although the elemental stiffnesses apparently converge quite well as a function of the model order, they are in error when compared to stiffnesses obtained from the known mechanical properties. The mean theoretical superelement stiffness for the three given sensor pairs is approximately 3.5×10^4 lb/in. The difference between the converged stiffness values identified from the data and the values known from the numerical example are due to the effects of modal truncation.

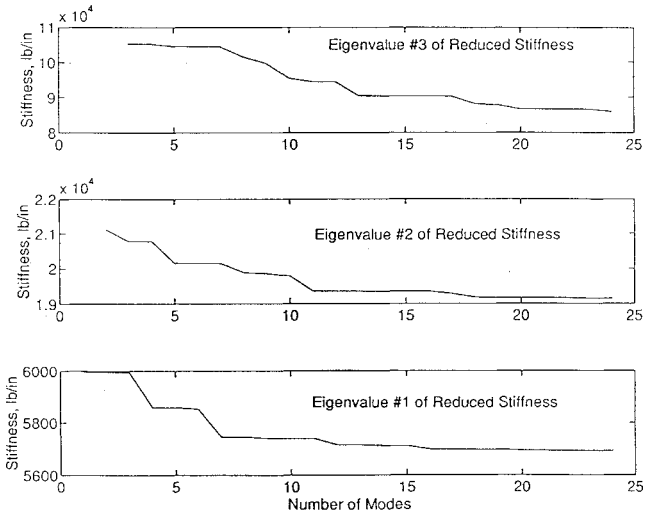

Fig. 7 Convergence of the reduced stiffness matrix.

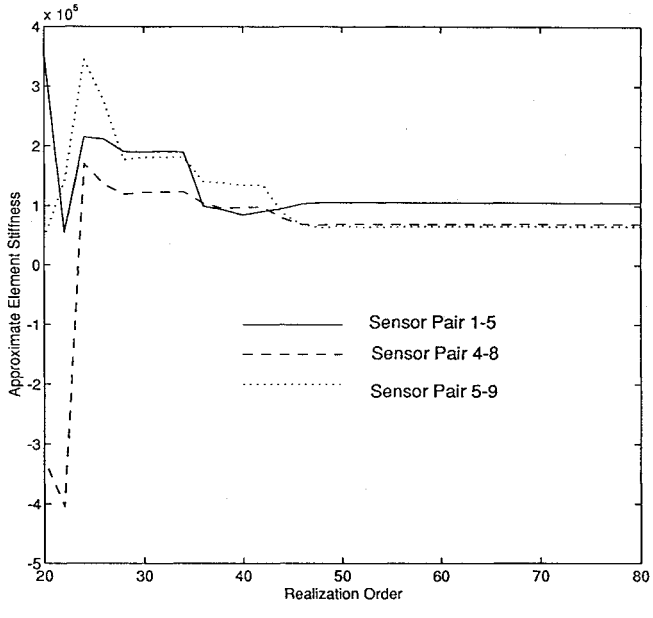

Fig. 8 Convergence of reduced element stiffnesses in planar truss.

C. Application to Experimental Data: Model Update and Damage Detection Experiment Modal Test

The methods described herein have also been applied to modal parameters derived from modal testing on the model update and damage detection experiment (MUDDE) testbed at the McDonnell Douglas Structural Dynamics and Controls Laboratory (SDCL) located at the University of Colorado, Boulder. The MUDDE structure is a 1/10 scale model of an eight-bay suspended segment of the Space Station Freedom truss structure, illustrated in Fig. 9. The testing was performed in the McDonnell-Douglas Aerospace Structural Dynamics and Controls Laboratory at the University of Colorado-Boulder. As part of research effort focusing on damage detection of space structures, transfer functions were obtained for three input forcing locations and 111 accelerometer outputs, using 30 trials to minimize the influence of noise. A fast version of the ERA algorithm[13] implemented on an IBM RS-6000 workstation was used to determine an approximate 500 state discrete-time realization for the 333 transfer functions. Each trial was sampled at 500 Hz for 16 s. From 247 complex-paired first-order poles plus six real first-order poles, 182 second-order mass-normalized modes were estimated by a variant of the CBSI algorithm. Approximate collocation of three output measurements to the three force inputs was used to appropriately scale the identified mode shapes.

In Fig. 10, a mesh plot of the calculated reduced stiffness $\bar{K}$ from the test data is shown. The stiffness matrix has an apparent

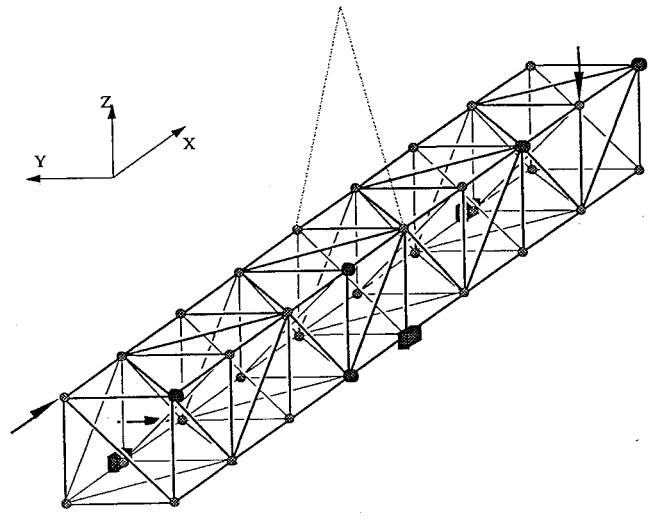

Fig. 9 MUDDE structure at the McDonnell Douglas Structural Dynamics and Controls Laboratory, University of Colorado, Boulder.

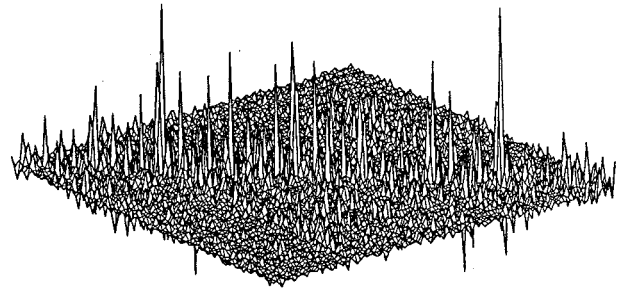

Fig. 10 Reduced measured stiffness matrix from MUDDE test.

diagonally-dominant topology, which is not imposed by the formula but presumably arises because of the numbering convention of the sensors (adjacent sensor number implied close physical proximity) and the mechanics of the structural design. The agreement of the measured stiffness connectivity with theory suggest that the approximate sensor to actuator collocation was sufficient to obtain a reasonable measure of the mass normalization of the modes. Minimum-order matrices were also successfully determined for the test data, as the number of identified modes exceeds the number of measured DOF by 71. Thus, it was determined that $\Delta\Omega$ had 71 nonzero singular values, and $\hat{K}$ and $\hat{M}$ were calculated, resulting in 71 real residual eigenvalues in Ω_r and the 111×71 mass coupling matrix M_c.

Because of computational restrictions, the convergence of the measured stiffness as a function of model order was not obtained. Instead, the CBSI-estimated normal modes were ordered by their modal singular values (MSV),[15] which is a measure of the modal contribution to the measured response. Modes with high MSVs will typically converge to stable modal parameters at relatively lower model orders. Using pairs of longitudinal direction sensors, the convergence of the measured stiffnesses of all 32 longeron members as a function of the number of participating modes is shown in Fig. 11. This is done in a manner equivalent to that of Fig. 8. The trend is generally similar to the numerical example, except that the modes are ordered from high to low MSV, so the modes added later on are more poorly identified (in general). This is not a problem if the flexibility contribution from that mode is relatively small. Low-frequency modes with low MSV values, on the other hand, can be problematic as seen in Fig. 11. The significant drop in the stiffnesses of four longeron elements seen around 120–130 modes is due to the addition of flexibility from mode 2. This mode has not only a low MSV and low frequency (relative to the overall modal spectrum), but also possesses a low modal phase collinearity[10] (indicating mode shape complexity and sensitivity to the mode shape estimation problem) and a low relative modal displacement at the driving points (which can affect the accuracy of the driving point modal scaling employed in this procedure). Therefore, given the low

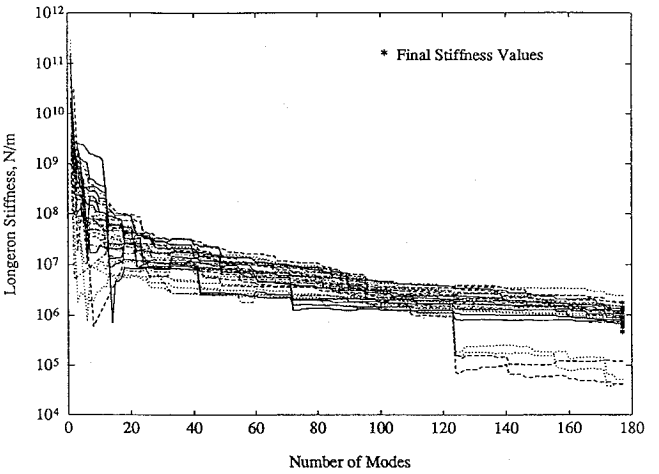

Fig. 11 Convergence of longeron stiffness for MUDDE truss modal test.

confidence in this modal contribution, the final undamped longeron stiffnesses were computed without including mode 2. These final stiffnesses are highlighted at the right-hand edge of Fig. 11.

VI. Conclusions

A generalized solution to the inverse vibration problem is presented for systems with arbitrarily small numbers of discrete physical sensors and arbitrarily large numbers of inherent natural modes. A condensation solution results in reduced physical matrices which possess asymptotic equivalence to the Guyan method for finite element model reduction. An equivalent minimum-order solution is obtained by augmenting the physical variable basis with generalized coordinates, resulting in a model which possesses the same topological properties as that obtained by the Craig-Bampton component mode synthesis method for dynamic finite element models. The resultant solutions have been applied successfully to numerical examples and experimental data.

The equivalent expression of modal properties through physical bases enables the efficient manipulation of such parameters to account for physical considerations such as substructure matrix assembly and boundary condition sensitivity, structural element damage detection, and model reduction for control using FEM-based methods. We plan to explore these applications in the near future.

Acknowledgments

The work reported herein was supported by a grant from NASA Langley Research Center, NAG-1-1200. The laboratory work was supported by a donation from the McDonnell-Douglas foundation and a donation from Shimizu Corporation. In addition, we would like to thank Charbel Farhat of Colorado University, Boulder, for much helpful feedback.

References

[1]Ewins, D. J., *Modal Testing: Theory and Practice*, Research Studies Press, 1984.

[2]Baruch, M., "Optimization Procedure to Correct Stiffness and Flexibility Matrices Using Vibration Tests," *AIAA Journal*, Vol. 16, No. 11, 1978, pp. 1209, 1210.

[3]Kabe, A. M., "Stiffness Matrix Adjustment Using Mode Data," *AIAA Journal*, Vol. 23, No. 9, 1985, pp. 1431–1436.

[4]Farhat, C., and Hemez, F., "Updating Finite Element Dynamic Models Using an Element-By-Element Sensitivity Methodology," *AIAA Journal*, Vol. 31, No. 9, 1993, pp. 1702–1711.

[5]Yang, C.-D., and Yeh, F.-B., "Identification, Reduction, and Refinement of Model Parameters by the Eigensystem Realization Algorithm," *Journal of Guidance, Control and Dynamics*, Vol. 13, No. 6, 1990, pp. 1051–1059.

[6]Hurty, W. C., "Dynamic Analysis of Structural Systems Using Component Modes," *AIAA Journal*, Vol. 3, 1965, p. 678–685.

[7]Guyan, R. J., "Reduction of Stiffness and Mass Matrices," *AIAA Journal*, Vol. 3, No. 2, 1965, p. 380.

[8]Craig, R. R., and Bampton, M. C., "Coupling of Substructures for Dynamic Analyses," *AIAA Journal*, Vol. 6, No. 7, 1968, pp. 1313–1319.

[9]Ho, B. L., and Kalman, R. E., "Effective Construction of Linear State-Variable Models from Input/Output Data," *Proceedings of the 3rd Annual Allerton Conference on Circuit and System Theory*, 1965, pp. 449–459; also, *Regelungstechnik*, Vol. 14, 1966, pp. 545–548.

[10]Juang, J. N., and Pappa, R. S., "An Eigensystem Realization Algorithm for Modal Parameter Identification and Model Reduction," *Journal of Guidance, Control, and Dynamics*, Vol. 8, No. 5, 1985, pp. 620–627.

[11]Vold, H., Kundrat, J., Rocklin, G. T., and Russell, R., "A Multiple-Input Modal Estimation Algorithm for Mini-Computers," Society of Automotive Engineers, *SAE Transactions*, Vol. 91/1, 1982, pp. 815–821; SAE Paper 820194.

[12]Alvin, K. F., and Park, K. C., "A Second Order Structural Identification Procedure via State Space-Based System Identification," *AIAA Journal*, Vol. 32, No. 2, 1994, pp. 397–406.

[13]Peterson, L. D., "Efficient Computation of the Eigensystem Realization Algorithm," Proceeding of the 10th International Modal Analysis Conf., Feb. 1992; *Journal of Guidance, Control, and Dynamics* (to be published).

[14]Peterson, L. D., and Alvin, K. F., "A Time and Frequency Domain Procedure for Identification of Structural Dynamic Models," *Proceedings of the AIAA/ASME/ASCE/AHS/ASCS 35th Structures, Structural Dynamics and Materials Conference* (Hilton Head, SC), AIAA, Washington, DC, 1994.

[15]Longman, R. W., Lew, J.-S., and Juang, J.-N., "Comparison of Candidate Methods to Distinguish Noise Modes from System Modes in Structural Identification," *Proceedings of the 1992 AIAA Structures, Structural Dynamics and Materials Conference* (Dallas, TX), AIAA, Washington, DC, 1992, pp. 2307–2317 (AIAA Paper 92-2518).